Available online at www.sciencedirect.com
ScienceDirect
Journal of Power Sources 171 (2007) 130–139
JOURNAL OF POWER SOURCES
www.elsevier.com/locate/jpowsour

Experimental simulation on the integration of solid oxide fuel cell and micro-turbine generation system

Wei-Hsiang Lai [a,*], Chi-An Hsiao [a], Chien-Hsiung Lee [b], Yau-Pin Chyou [b], Yu-Ching Tsai [b]

[a] *Institute of Aeronautics and Astronautics, National Cheng Kung University, Tainan 701, Taiwan, ROC*
[b] *Institute of Nuclear Energy Research, Atomic Energy Council, Taiwan, ROC*

Received 20 October 2006; accepted 7 November 2006
Available online 18 December 2006

Abstract

Solid oxide fuel cell (SOFC) is characterized in high performance and high temperature exhaust, and it has potential to reach 70% efficiency if combined with gas turbine engine (GT). Because the SOFC is in developing stage, it is too expensive to obtain. This paper proposes a feasibility study by using a burner (Comb A) to simulate the high temperature exhaust gas of SOFC. The second burner (Comb B) is connected downstream of Comb A, and preheated hydrogen is injected to simulate the condition of sequential burner (SeqB). A turbocharger and a water injection system are also integrated in order to simulate the situation of a real SOFC/GT hybrid system. The water injection system is used to simulate the water mist addition at external reformer.

Results show that this configuration can simulate the SOFT/GT hybrid system successfully. Water mist addition will increase the GT rotational speed, but an optimal amount exists during the variation of water injection. In residual fuel addition test, hydrogen shows good combustion efficiency and preheating temperature is the dominant parameter for hydrogen burning in SeqB even without flame holding mechanism in it. When preheating temperature is among 450–600 °C, hydrogen will have almost 100% combustion efficiency at 90% engine loading, and GT will get a higher rotational speed for the same energy input. But when the engine operates at 100% loading, the combustion efficiency will decrease while fuel utilization (U_f) setting is increasing. When raising the preheated temperature to 650–700 °C, the combustion efficiency will increase rapidly.

Keywords: Solid oxide fuel cell; SOFC; Hybrid system; Micro gas turbine; Sequential burner

1. Introduction

Recently, the studies about fuel cell are most focused on PEMFC, DMFC and SOFC, and each of them has their own advantages and disadvantages. Among those fuel cells, SOFC has the advantages of high performance and high temperature exhaust gas.

In general, the efficiency of SOFC itself is about 45–65% [1], but if its high temperature exhaust gas is introduced to gas turbine engine, the potential of power generation will rise to about 70%, which is higher than traditional compound cycle (40–60%). It is called SOFC/GT hybrid system if combined SOFC with gas turbine. If SOFC is combined with co-generation system, the total efficiency will attain to 80–85% [2,3].

After the concept of SOFC/GT hybrid system was proposed at early 1990, there were several articles further discussing its application. However, most of papers are dealing with theoretical cycle analysis and simulation of the possible configuration of hybrid system. Palsson et al. [4] conducted theoretical studies of combined SOFC and gas turbine (SOFC/GT) cycles to evaluate its performance prospects. Its reference system was sized at 500 kW, so that gas turbine reheat and air compression intercooling were also included in analysis. The results showed that pressure ratio has a large impact on performance, and electrical efficiency can be more than 65% even at low pressure ratio.

Massardo et al. [5,6] developed a completed mathematical model of SOFC/GT system. They worked on thermodynamic analysis of whole system and estimated the economic benefits. That model is suitable for discussing systems using internal reforming. In that paper, it provided composition estimation model for estimating SOFC exhaust residual fuel and discussed the effects on SOFC/GT system, for example, fuel air ratio

* Corresponding author. Tel.: +886 62082848; fax: +886 62389940.
E-mail address: whlai@mail.ncku.edu.tw (W.-H. Lai).

0378-7753/$ – see front matter © 2006 Elsevier B.V. All rights reserved.
doi:10.1016/j.jpowsour.2006.11.017

Nomenclature

APH	air preheating
DMFC	direct methanol fuel cell
E	input energy
FAR	fuel air ratio
GT	gas turbine
HAT	humid air turbine
MGT	micro gas turbine
P_3	compressor outlet pressure
PEMFC	polymer electrolyte membrane fuel cell
ΔR	rotational speed difference
S/C	steam to carbonate ratio
SeqB	sequential burner
S/M	steam to methane ratio
SOFC	solid oxide fuel cell
SOFC/GT	solid oxide fuel cell/gas turbine hybrid system
STIG	steam injected gas turbine
$T_{f\text{-}2}$	preheated hydrogen temperature
$T_{3\text{-}1}$	compressor outlet temperature
$T_{3\text{-}2}$	combustor inlet temperature
$T_{4\text{-}1}$	first combustor outlet temperature
$T_{4\text{-}2}$	second combustor outlet temperature
T_5	first turbine outlet temperature
U_f	fuel utilization efficiency
Y	difference of energy value

(FAR), fuel inlet composition, and operation pressure and so on. Costamagna et al. [7] studied the design and off-design analysis of a hybrid system (SOFC/GT) with size (250/300 kWe), and the results showed more than 60% at both design and off-design if gas turbine well regulated by variable speed control. Winkler and Lorenz [3] also showed that the combined fuel cell cycle may reach an electrical efficiency more than 80% by reheat (RH)-SOFC-GT-ST cycle.

In 2003, Kuchonthara et al. [8] evaluated several enhanced gas turbine cycles with the combinations of solid oxide fuel cell, in addition to conventional GT system, steam injected gas turbine (STIG) cycle, steam turbine (ST), and humid air turbine (HAT) were also considered. Moreover, additional recuperation by air preheating (APH) in STIG cycle is also included. They concluded that the combination of SOFC-HAT cycle yields the highest overall efficiency. The humid air in GT system deserves to further study in this area.

Although the SOFC system is under developing and its reliability still need to further improvement, there are a lot of topics on the GT and the system integration to be investigated concurrently. However, not many papers are found to approach these problems by the experimental work, except some research company. The SOFC is still too expansive for the research in the university; The authors consider that the sequential burner (SeqB) which combines SOFC outlet with GT inlet is one of key components in SOFC/GT system. The fuel utilization efficiency (U_f) of SOFC is about 65–85%, it means there is about 15–35% of total fuel unused. So, the utilization of SeqB is to burn the residual fuel and to increase exhaust gas temperature to maintain the speed of gas turbine. In order to understand the performance of SeqB thoroughly, the authors simulate the operation condition of SeqB of SOFC/GT system by experimental method and observe the reaction of residual fuel and its effect on GT performance.

2. Approach methodology

2.1. System conceptual design

In general, the power generation ratio of SOFC and GT is 3:1 to 5:1 in a typical SOFC/GT system. The power generation of micro turbine power systems nowadays are ranged on 15–50 kW. If one chooses the most common power generation ratio of SOFC/GT system, the power capacity of SOFC in micro SOFC/GT system is at least 45 kW. Because the real SOFC is not available at this stage, the authors design a SOFC/GT system by using a traditional combustor (Comb A) to simulate SOFC exit condition, and followed by another combustor (Comb B) which simulate the sequential burner to allow additional hydrogen injection for complete combustion of residual unburned gas from SOFC. A turbocharger and a water injection system are also integrated in order to simulate the situation of a real SOFC/GT hybrid system. The water injection system is used to simulate the water mist addition at external reformer. From such a simulated system, the cost of experiment will significantly reduced, and the studies of many problems in the system integration of gas turbine, and power generation will be possible at this stage.

2.2. Theoretical analysis

To simulate SOFC exit condition by using a traditional combustor, one should clearly know the differences between SOFC/GT hybrid system and traditional GT. The concept of SOFC/GT hybrid system can be recognized as replacing combustor by SOFC in traditional GT system. But there are still some differences: (1) fuel reaction mechanism; (2) fuel/air ratio, FAR; (3) fuel composition. Regarding to fuel reaction mechanism, for example, in SOFC/GT system, the fuel reaction is dominated by electrochemistry reaction, but in GT system, fuel reaction is totally chemical reaction (combustion). However, the total reaction is the same, and can be expressed as methane reaction (Eq. (1)):

$$CH_4 + 2O_2 \rightarrow CO_2 + 2H_2O \quad (1)$$

The FAR is lower in GT than that in SOFC/GT system. For fuel composition, natural gas is usually used in SOFC/GT. In order to increase reaction rate, natural gas is usually reformed to hydrogen rich gas through a reformer. If using steam reforming reaction, water steam must be added to system in the reforming process and its mass ratio is about 1.5–2.5 times of methane [9]. High water addition might affect the efficiency of original GT performance. From the view point of energy, the fuel totally releases energy in GT system, and this energy is used to raise gas temperature in combustor except heat

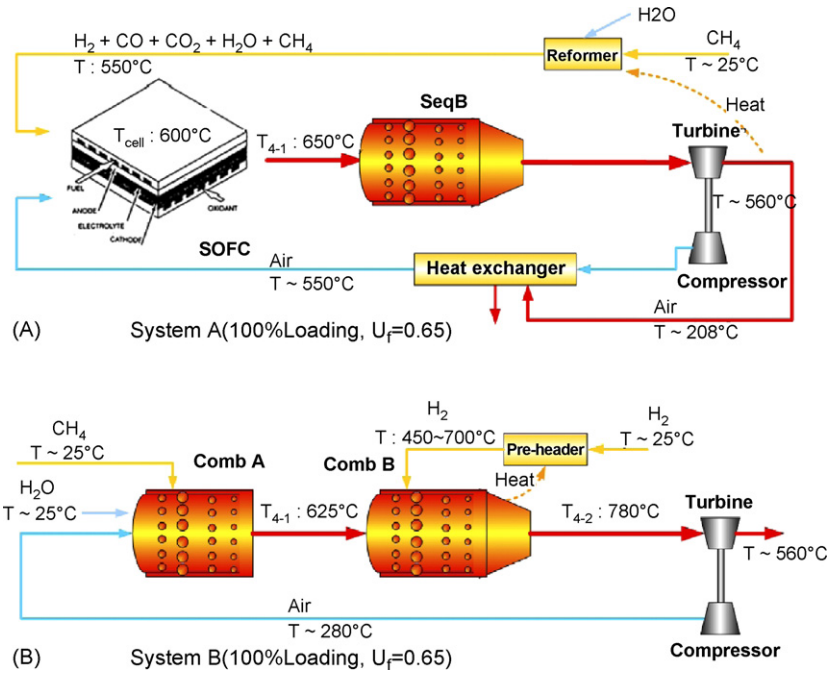

Fig. 1. Conceptual simulation of system, (A) SOFC/GT system, and (B) simulated system.

loss. But in SOFC/GT hybrid system, the most fuel energy is released in electrical power; residual energy is released in heat because of internal resistance of SOFC. This heat is not only used for maintaining SOFC temperature, but also for internal reforming in SOFC and water steam shift reaction. Some other heat is to raise the temperature of product and air before the exit.

From above overview, if we can find a GT which FAR is similar to SOFC/GT, and turbine inlet temperature near SOFC/GT operation condition, then the combustor exit temperature and gas composition will be similar to SeqB exit condition in real SOFC/GT hybrid system. Based on above concept, specific SOFC/GT operation condition can be simulated by using two combustors (one for SOFC, the other for SeqB), a turbocharger, water mist addition device, and fuel control system. Besides, the effects on gas turbine engine of water mist addition and residual fuel flow for combustion can also be discussed.

2.3. System integrated analysis

The chosen SOFC/GT hybrid system is presented in Fig. 1, including setup an original SOFC/GT system (system A) as the goal to be simulated and a simulated system after replacing the SOFC by a combustor (system B) used to experimental simulation. In system A, there are SOFC, SeqB, GT, reformer, and heat exchanger. In this study, the main goal is the preliminary study of this concept verification, and focus on the SOFC exit to turbine inlet, so the parameters of reformer and heat exchanger are not discussed. The inlet and exit conditions are provided by ENER which was also published on Chyou's paper [10].

The original operation process (system A) is described as follows: the compressed air (about 208 °C) which comes from compressor is heated to 550 °C by high exhaust gas from turbine and then enters SOFC cathode. Fuel (CH_4) is proceeded through reforming reaction with steam supplied into reformer before entering SOFC anode. The reforming ratio is about 30% of total fuel, and steam to carbonate ratio (S/C) is 2.89, set temperature is 550 °C. In many references of numerical simulation, temperature of fuel cell is set as constant to reduce difficulties during analyzing. In this study, we refer to heat transfer analyzing model in reference [10], and assume SOFC exit gas temperature to increase about 100 °C, so mean operation temperature of SOFC is setting 600 °C. There are different amount of residual fuel gas at the exit of SOFC due to different fuel utilizing ratio, and it can be burned completely by SeqB theoretically before coming into the gas turbine.

This experimental simulation system (system B) is setup by adding a residual fuel combustor (Comb B) behind the original combustor (Comb A). The function of Comb A is to create similar conditions, both high temperature and most of ingredients (CO_2, H_2O) at SOFC exit; Comb B is equivalent to a SeqB of system A and main composition (H_2) of residual fuel is accessed in this system.

The operation process of system B is also described as follows: the compressed air (about 208 °C) comes from compressor exit is mixing with plenty of water mist, which is atomized by atomization device, before entering Comb A. This is to simulate additional water in reformer of system A. The fuel, methane, is added into combustor A to burn under the condition without preheated, and its mole number is the same as the SOFC exit CO_2 under specific fuel utilizing ratio of system A. That is because the total fuel reaction equation in SOFC is just the same as methane oxidization reaction, so we can do this to simulate the fuel composition reacted inside SOFC. The high temperature gas come from Comb A then enter Comb B, and preheated H_2 is added in Comb B to simulate residual fuel reaction in SeqB of system

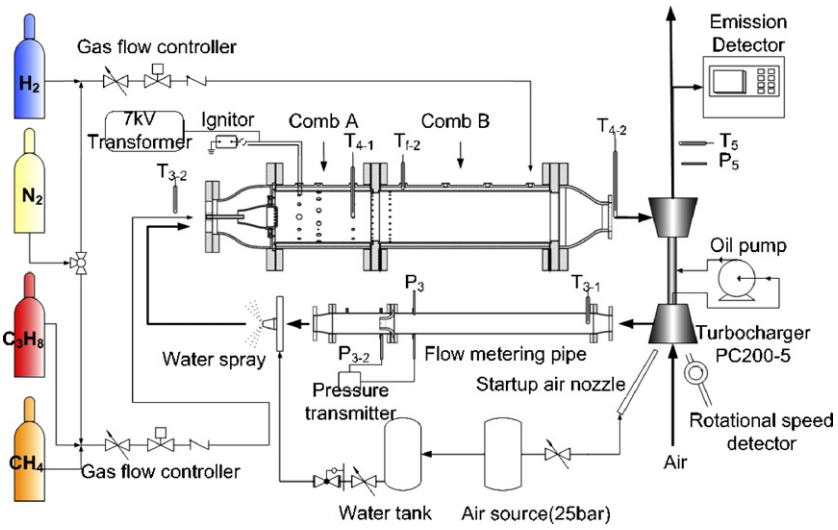

Fig. 2. Schematic of experimental setup.

A. The reacted gas then push turbine, and drive compressor to breathe fresh air and proceed system cycling.

3. Experimental setup

The experimental setup in this study consists of an SOFC exit simulation combustor (Comb A), a residual fuel combustion simulation burner (SeqB or Comb B), a turbo-charger, flow rate measurement pipe, mist generation device, and so on. The facilities layout is shown in Fig. 2. The function of each facility and design concept described as follow.

3.1. Combustors

There are two combustors in this study, i.e., Comb A and Comb B, and their structures are shown in Fig. 3. As described previously, Comb A is used for system starting and simulating SOFC exit condition and its length is 27.5 cm. Comb B is a residual fuel simulation burner, and it is used to burn preheated hydrogen, and its length is 60 cm.

Comb A is a can type combustor, its design concept comes from the methane combustor in reference [11] with some modifications. Its structure includes fuel premixing zone, radial swirler, and liner. In order to know the hydrogen reaction circumstance in SeqB under different fuel utilizing rate, a hydrogen reaction circumstance is designed in high temperature environment but under no special flame holding device condition. Comb B (Fig. 4) is designed to simulate a SeqB in SOFC/GT hybrid system. The simulating residual fuel, hydrogen, is injected from rear section of SeqB, and passes through the channel between outer casing and liner. In this passage, the high temperature liner wall should preheat hydrogen. Finally, hydrogen is injected into liner radially from 24 holes and its diameter 4 mm in front section of Comb B, and burned with high temperature gas from Comb A.

3.2. Turbocharger

A turbocharger in this study is provided by Chiau-Cheng Co., its model number is PC200-5. The compressor and turbine are both centrifugal type. Its original design point performance can provide up to 0.18 kg s^{-1} air with pressure ratio 3.1, as shown in Table 1. This turbocharger is originally designed for truck diesel engine to provide more air flow and higher pressure to get more power output. But in this study, it plays the role as a GT in system B.

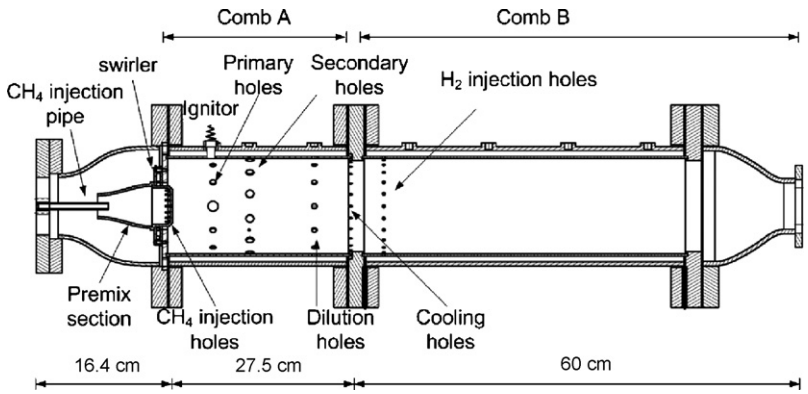

Fig. 3. Schematic of combustor.

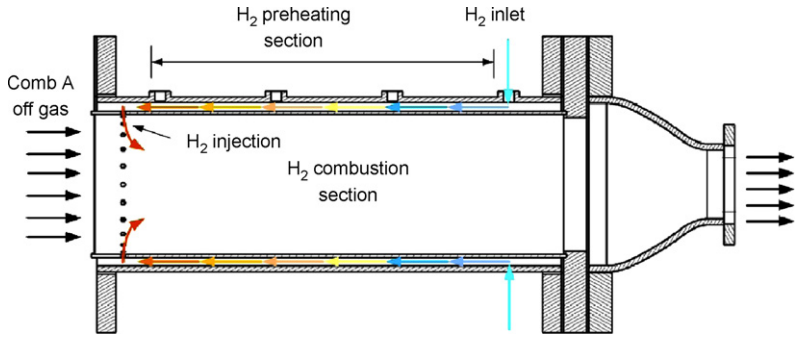

Fig. 4. Comb B structure and its operation.

Table 1
Design point performance of turbocharger

Model no.	Air flow rate (kg s^{-1})	P ratio	Maximum speed (rpm)	Maximum temperature (°C)
PC200-5	0.182	3.1	130,000	760

Table 2
Test matrix of studies

Loading (%)	Preheated temperature (°C)	$U_f = 0.65$	$U_f = 0.75$	$U_f = 0.85$
100	450–600	Case 1a	Case 2a	Case 3a
90	450–600	Case 6a	Case 5a	Case 4a
100	650–700	Case 1b	Case 2b	Case 3b
90	650–700	Case 6b	Case 5b	Case 4b

3.3. Water mist generation device

The mist injection is located on rear section of flow measuring pipe. In order to enhance the evaporation and avoid the accumulation of the water at the bottom of piping, a pressure type spray nozzle is chosen to atomize liquid water, and its model is 1/4MKB80071S303 produced by IKEUCHI, Japan. The spray nozzle has a hollow cone pattern with spray angle 80°, the operation pressure is about 7 kg cm^{-2}, and its Sauter Mean Diameter of spray is about 90 μm.

3.4. Apparatus

The apparatus include fuel control system, sensors, and DAQ systems. Fuel control system includes two Dwyer GFC-series flow controllers for methane, and hydrogen, respectively, and their errors are both ±1.5% FS (full scale). There are two kinds of pressure transducer used in this study. One is gage pressure transducer with rated range 0–6 bar and accuracy ±0.15% FS to measure static pressure of compressor exit and first turbine exit. The other is differential pressure transducer with range is 0–5 psid and accuracy ±0.25% FS to measure flow rate. Tachometer system includes two components, i.e., magnetic sensor and signal receiving indicator. The ACT-3 indicator rated range is 0–999,990 rpm pulse signal and magnetic sensor rated range is 500,000 rpm. Temperatures are measured by K-type thermocouple, both temperature and pressure measuring positions are shown in Fig. 2. $T_{3\text{-}1}$ represents compressor outlet temperature; $T_{3\text{-}2}$ is combustor inlet temperature; $T_{4\text{-}1}$ is the temperature of first combustor outlet (the real position lie on liner dilution hole); $T_{4\text{-}2}$ is the temperature of second combustor outlet; $T_{f\text{-}2}$ locates near hydrogen nozzle outlet, and represents preheated hydrogen temperature; T_5 represents first turbine exit temperature; P_3 represents compressor outlet pressure.

The DAQ system is provided by National Instrument, including a SCXI and NI 6024E data acquisition card, and the Labview software. All sensors response can be connected to a personal computer to record it at the rate of 5 Hz, and to monitor the situation of the test.

The above-mentioned set up is established to simulate the SOFC/GT integration system, and the text matrix of this study is shown in Table 2.

4. Results and discussion

4.1. Basic performance test of GT

Because pure methane is expensive, long time operation is not affordable. In order to get long time operation, propane (C_3H_8) is used to start system and warm up about 120 s, then gradually switches to methane fuel. The basic performance test procedure is shown as Fig. 5. This experiment is also the test of the fuel switching to gain the experience of operation, and verify the above-mentioned concept of the system integration. The turbine speed can be operated as high as 130,000 rpm that means this system can work well as it can get to the design point operation.

4.1.1. Water mist addition test

The effect on GT of water mist addition is represented by temperature change of each section. Taking Fig. 6 for exam-

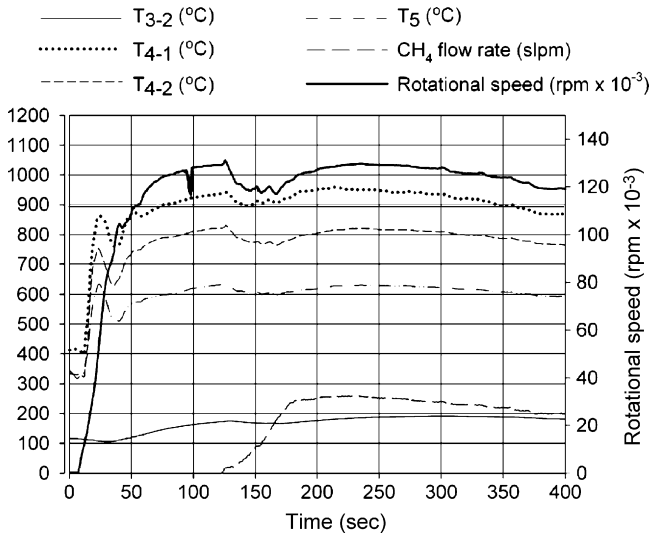

Fig. 5. Basic performance test of methane fuel.

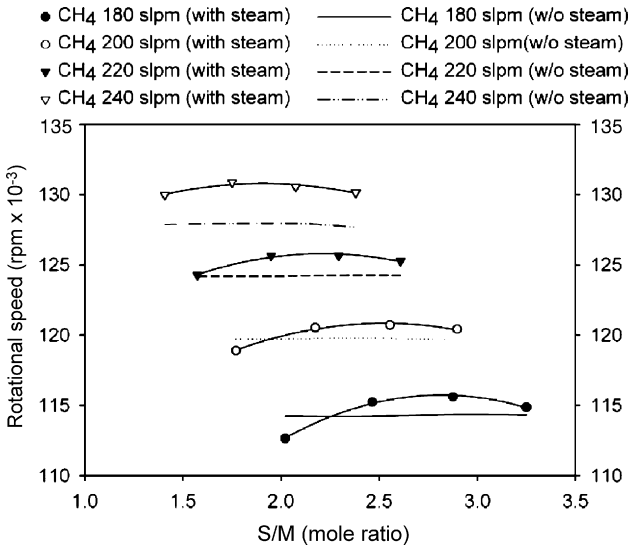

Fig. 7. Steam-to-methane ratio to engine speed.

ple, the test method is maintaining constant water pressure at 7 kg cm^{-2} and increasing methane flow rate from 180 to 240 slpm. From Fig. 6, it is found that $T_{4\text{-}1}$, $T_{4\text{-}2}$, and T_5 decrease clearly due to water mist addition. The temperature decrease will make simulated SOFC exit temperature lower to 625–650 °C.

Although turbine temperature decreases, rotation speed does not decrease simultaneously. Fig. 7 shows rotation speed change with different water mist flow under the condition of different methane flow rate. To distinguish from S/C of SOFC/GT system, steam to methane ratio (S/M) is used as an analyzing parameter. From Fig. 7, it is shown that there exists an individual optimal S/M to reach the highest rotation speed increase in different methane flow rates. The higher methane flow rate, the more rotation increase, and the S/M range of rotation speed increase are wider. Observing real water steam flow rate in Fig. 8, it shows there exist highest rotation speed increase when water flow rate is between 5.75 and 6.25 kg s^{-1}.

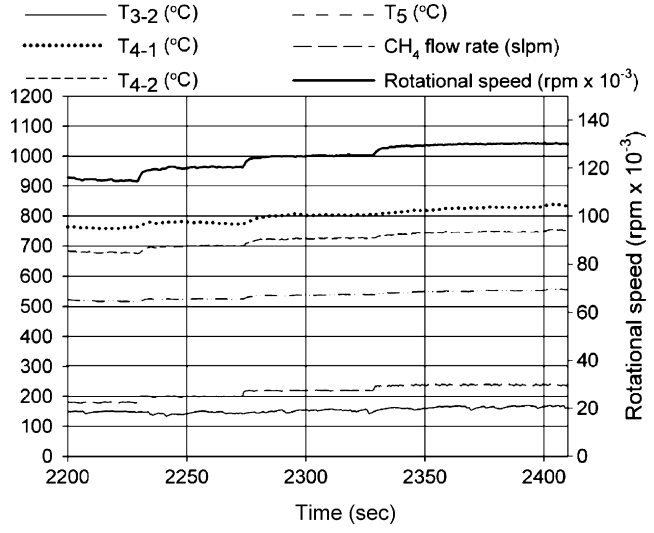

Fig. 6. Performance test of water mist addition.

4.2. Results of residual fuel addition test

Test of residual fuel addition is simulated according to the fuel composition obtained from the theoretical calculation. The goal of test is to observe the reaction of hydrogen in residual fuel in $U_f = 0.65$, 0.75, and 0.85 cases which under the conditions of 90% loading and 100% loading. Fig. 9 is the experimental procedure of residual fuel addition test, and the numbers in that figure represent different simulating target.

Comparing $T_{4\text{-}1}$ and $T_{4\text{-}2}$ in Fig. 6 with Fig. 9, it is found that $T_{4\text{-}1}$ is nearly the same as $T_{4\text{-}2}$ because of hydrogen addition in Comb B and methane subtraction in Comb A. In fact, the temperature of Comb A exit should be 100 °C lower than $T_{4\text{-}1}$; which is close to $T_{4\text{-}2}$ as in Fig. 6, because there is a row of dilution holes just located after $T_{4\text{-}1}$; so actual temperature of Comb A is about 600–700 °C and similar to the condition of system B in theoretical computation. Fig. 10 shows the variation

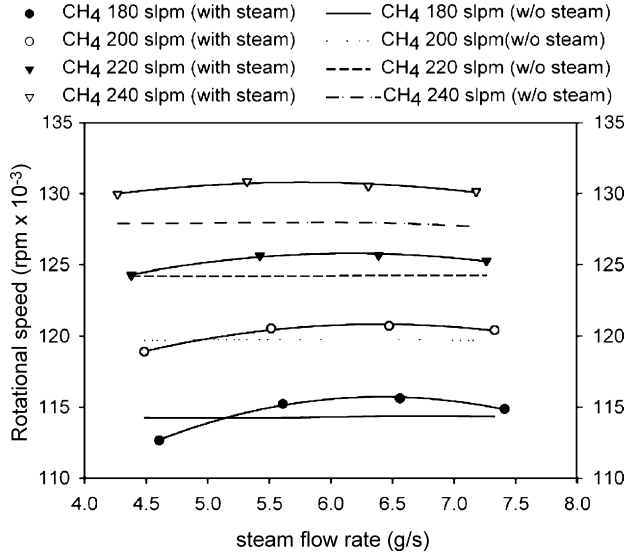

Fig. 8. Steam flow rate and rotational speed.

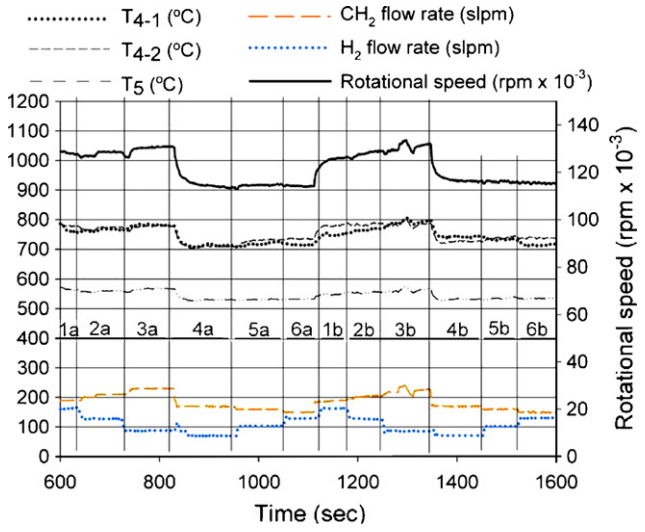

Fig. 9. History of residual fuel addition.

of hydrogen preheated temperature before entering into Comb B which is raised from 450 to about 700 °C during the experiment operation. This variation is resorted to hydrogen preheating device, from Fig. 4, the preheating of hydrogen is transferred by convection heat comes from liner wall of Comb B.

In order to asses the change of system performance after adding residual fuel (hydrogen), it is discussed from the view point of energy. This method is to compare the performance difference (rotational speed, consumption of fuel) of water mist addition test and residual fuel addition test. In the residual fuel addition test, there is a specific water input (x axis) versus measured rotation speed (y axis) in each case with different loading and U_f. So it appears a single point in the water mist addition test performance graph of each case. By comparing input energy (E), i.e., methane energy, hydrogen energy, and hydrogen preheat energy, that offered in each case actually with the energy (X) (methane energy only) needed to provide while reaching the same rotational speed, we can know the performance difference with residual fuel addition. Here we define the difference of

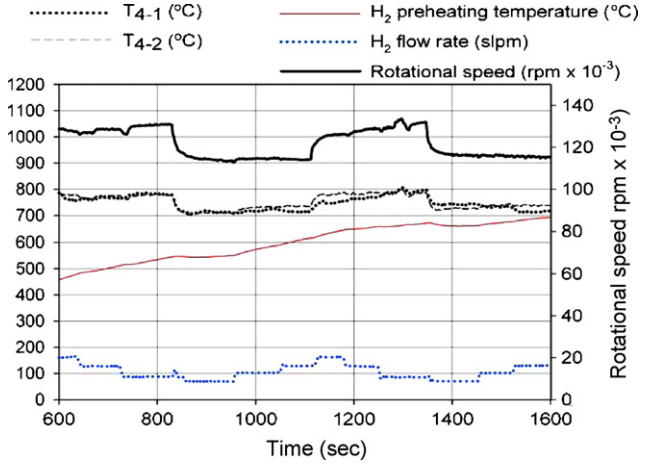

Fig. 10. History of preheated hydrogen.

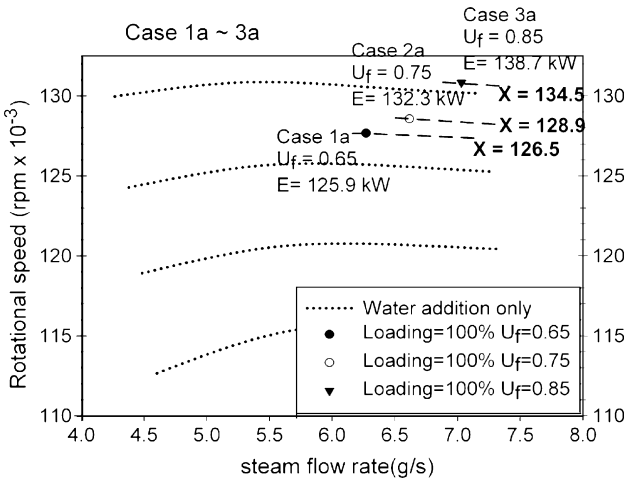

Fig. 11. Comparison in residual fuel and water mist addition (1).

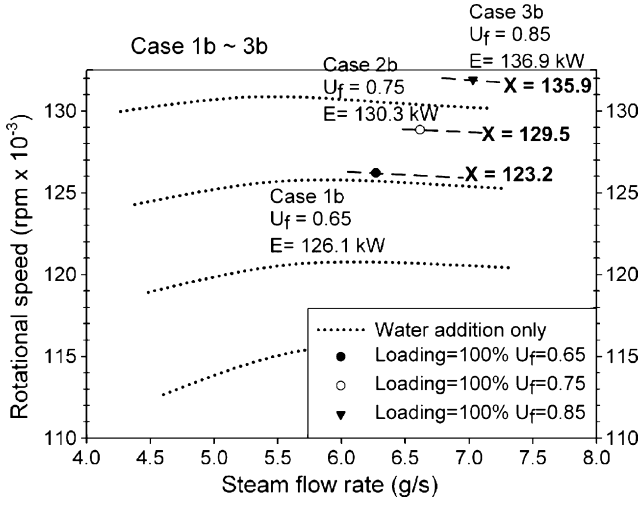

Fig. 12. Comparison in residual fuel and water mist addition (2).

energy (Y)

$$Y = E - X \tag{2}$$

where E is the actual energy supplied to the system, and X is the energy need to provide alternatively by methane and/or the adding of water mist.

From Table 3, it can be observed that the influence of the system energy utilization while hydrogen is added, but it is difficult to find out the impact on system loading. So, the input energy (E) in each case of residual fuel addition test can be recognized as a baseline to gain an equivalent rotation speed R_1, and under the condition of providing the same energy (E), a new rotation speed R_2 can be reached after water mist addition. By comparing the rotational speed variation (ΔR) between these two conditions, then divided by R_2, it is clearly to see the rotation speed increase percentage of GT of residual fuel addition. The result is shown in Table 4.

The comparison graphs can be plotted from Figs. 11–14 of residual fuel addition and water addition test by using the data of Table 3. The thin dotted lines in the figures are the results of water mist addition tests; every curve shows the rotational

Table 3
Energy balance of residual fuel and steam addition test

Test no.	Preheating temperature (°C)	L (%)	U_f	Speed (rpm)	Energy supplied E (kW)	Steam addition energy X (kW)	Energy balance Y (kW)	Up/down
Case 1a	450–600	100	0.65	127,678	125.89	126.46	−0.57	↓
Case 2a	450–600	100	0.75	128,574	132.30	128.93	+3.37	
Case 3a	450–600	100	0.85	130,845	138.66	134.47	+4.19	
Case 4a	450–600	90	0.85	113,866	103.05	99.1	+3.95	↑
Case 5a	450–600	90	0.75	114,888	101.68	102.61	−0.93	
Case 6a	450–600	90	0.65	114,043	99.38	102.6	−2.80	
Case 1b	650–700	100	0.65	126,204	126.09	123.15	+2.94	↑
Case 2b	650–700	100	0.75	128,853	130.34	129.53	+0.81	
Case 3b	650–700	100	0.85	131,909	136.88	136.97	−0.09	
Case 4b	650–700	90	0.85	116,104	103.40	103.25	+0.15	↑
Case 5b	650–700	90	0.75	115,845	101.90	104.30	−2.40	
Case 6b	650–700	90	0.65	115,314	99.29	104.61	−5.32	

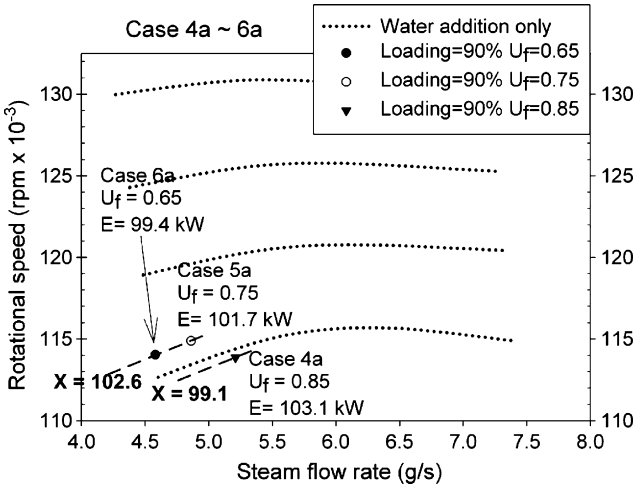

Fig. 13. Comparison in residual fuel and water mist addition (3).

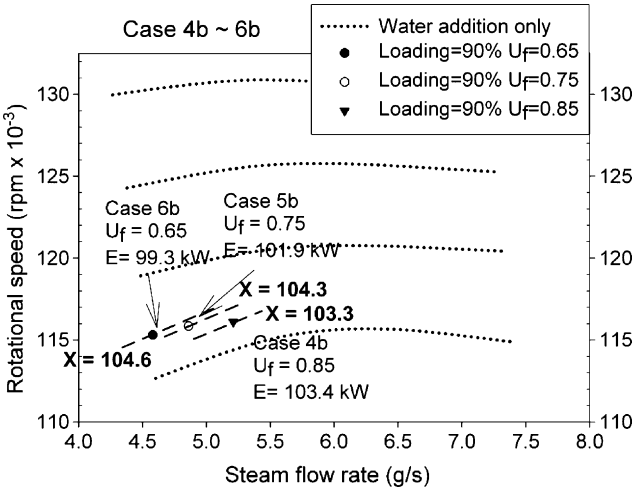

Fig. 14. Comparison in residual fuel and water mist addition (4).

Table 4
Speed in residual fuel and water mist addition

Test no.	Preheating temperature (°C)	L (%)	U_f	Speed R_1 (rpm)	Speed (after mist) R_2 (rpm)	ΔR ($R_1 - R_2$) (rpm)	Increase speed $\Delta R/R$, (%)	Up/down
Case 1a	450–600	100	0.65	127,678	127,431	+247	+0.19	↑
Case 2a	450–600	100	0.75	128,574	130,076	−1502	−1.15	
Case 3a	450–600	100	0.85	130,845	132,658	−1813	−1.37	
Case 4a	450–600	90	0.85	113,866	115,973	−2107	−1.82	↓
Case 5a	450–600	90	0.75	114,888	114,404	+484	+0.42	
Case 6a	450–600	90	0.65	114,043	112,178	+1864	+1.67	
Case 1b	650–700	100	0.65	126,204	127,519	−1315	−1.03	↓
Case 2b	650–700	100	0.75	128,853	129,203	−350	−0.27	
Case 3b	650–700	100	0.85	131,909	131,890	+19	+0.01	
Case 4b	650–700	90	0.85	116,104	116,183	−79	−0.07	↓
Case 5b	650–700	90	0.75	115,845	114,515	+1330	+1.16	
Case 6b	650–700	90	0.65	115,314	112,155	+3159	+2.28	

speed change (y axis) versus water mist addition amount under the condition of providing the same fuel energy (x).

One can observe detailedly from Fig. 11, when the engine is in 100% loading, preheating temperature is 450–600 °C, it is found that system performance is decreasing (Y is negative value) in higher U_f condition except for $U_f = 0.65$. According to rotation speed increase percentage, when U_f is 0.65, its rotation speed increase percentage is +0.19%, but when U_f increases to 0.85, its rotation speed increase percentage changed to negative value (−1.37%). And the trend above shows that when the amount of the hydrogen in the gas flow is higher (U_f is lower), the system will reveal better performance under water mist addition. Then observe Fig. 12, when the engine is in 100% loading, preheating temperature is 650–700 °C. It is found that the performance reduction is not as much as in Fig. 11 in the state of U_f is of 0.75 and 0.85. But comparing Case 1a with Case 1b, Y value increase from −0.57 to +2.94%; the rotational speed variation percentage from +0.19 to −1.03%, this is because the data acquired is under the unsteady condition in that test. From Fig. 9, it is found that the rotation speed is in the increasing trend (the same as Case 2b), so the rotation speed can be reached in Case 1b and Case 2b should be higher. Estimating Case 1b and Case 2b by the trends of Case 1a–3a, their Y values should be smaller than Case 3b and the values are negative.

Fig. 13 shows the reaction circumstance under the condition of 90% engine loading and 450–600 °C preheated temperature. It is found that Y value decrease with U_f increase, and the trend is the same as the condition of 100% loading. Fig. 14 shows the reaction circumstance under the condition of 90% engine loading and 650–700 °C preheated temperature. Comparing with Fig. 12, it is also shown that the increase of preheated temperature will benefit in reducing Y value. In Case 4b–6b, almost all cases have negative Y value, and shows decrease of energy consumption. This phenomenon represents not only good combustion of hydrogen in the sequential burner, but also slightly increasing system performance. Finally, regarding to the difference of 90% and 100% loading conditions; it is found that, when U_f is higher and under different preheated temperature conditions, the rotation speed increase of 90% loading condition is higher. Because the operation conditions and settings are different in 90% and 100% loading, so we cannot proceed performance comparison.

From the above discussion, it is known that the result of residual fuel will affect deeply by preheated temperature. And the Y value of 90% engine loading is lower than that of 100% engine loading. The reason maybe that when in lower loading, the velocity of main flow is lower, so hydrogen can have longer residence time. Speaking of the effect on Y value and rotation speed increase of U_f, it is shown that when U_f is higher, Y value will become higher and rotation speed increase become lower. It is easy to see that when hydrogen flow rate is lower in higher U_f condition, the hydrogen concentration of Comb A exhaust is relative low, so hydrogen maybe diluted to flammable limit by main flow, and make incomplete combustion and lower combustion efficiency. In some cases, Y value appears with negative value (energy saving), the reason maybe as follow: first, the hydrogen addition can promote micro-methane to react further, and make the same rotation speed in water addition test with lower fuel providing. Another possible explanation is like Jin and Ishida [12], who do the dilution gas addition test in H_2/O_2 GT system. Comparing the effect of N_2 and water addition: because the produce of H_2/O_2 combustion is water, so if we use water steam as dilution gas, it can reduce energy loss by multi-components mixing. In this study, we add water in air which has existed, so the effect should be between Jin model and real GT system, so there is possibility to increase system efficiency.

5. Conclusions

1. It is successful to demonstrate the possibility by utilizing two combustors and a turbocharger to simulate the approximate condition of a SOFC/GT system which is operated with FAR similar to intended SOFC/GT hybrid system.
2. From water mist addition test, it is found that water mist addition can increase on GT rotation speed increasing. Due to channel size, there exists an optimal value of water mist addition rate. Too much more or too less than its optimal amount will decrease rotation speed raise, even worse condition than without water mist addition. In higher rotation speed condition, water mist addition range which can increase on rotation speed raise is wider.
3. In this study, hydrogen is injected to combustor radially. It is found that combustion efficiency is good even in the condition without specific flame holding device, and higher hydrogen combustion efficiency can be got in lower engine loading condition.
4. From comparison of differential hydrogen preheated condition, it is found that hydrogen has excellent combustion efficiency under the condition of 450–600 °C preheated temperature at 90% loading, and they will increase rotation speed. When loading is 100%, the combustion efficiency is decreasing when U_f is increasing, even decrease system performance. When preheated temperature is between 650 and 700 °C, hydrogen combustion efficiency will increase clearly under all test conditions, and we can get higher rotation speed with lower energy providing.
5. In such a SOFC/GT hybrid system, if the SOFC belongs to high temperature type (800–1000 °C), it needs not specific device to burn hydrogen. But for a mid-low temperature type (500–800 °C), it needs better mixing and flame holding device to handle residual fuel if the temperature is lower.

Acknowledgements

The authors acknowledge the financial support from Institute of Nuclear Energy Research (INER), Taiwan, under the contract 95 2001 INER 050, and from Energy Bureau of Ministry of Economic Affairs, Taiwan under contract no. 95-D0137-5 to make this research successfully. The hardware support of turbo-charger from Chiau-Cheng Co. is also appreciated.

References

[1] US DOE, Fuel Cell Handbook, sixth ed., EG&G Services Inc., West Virginia, 2002.
[2] S. Veyo, Westinghouse Fuel Cell Combined Cycle Systems, Westinghouse Science & Technology Center, 1997.
[3] W. Winkler, H. Lorenz, J. Power Sources 105 (2002) 222–227.
[4] J. Palsson, A. Selimovic, L. Sjunnesson, J. Power Sources 86 (2000) 442–448.
[5] A.F. Massardo, F. Lubelli, J. Eng. Gas Turbine Power 122 (2000) 27–35.
[6] A.F. Massardo, L. Magistri, J. Eng. Gas Turbine Power 125 (2003) 67–74.
[7] P. Costamagna, L. Magistri, A.F. Massardo, J. Power Sources 96 (2001) 352–368.
[8] P. Kuchonthara, S. Bhattacharya, A. Tsutsumi, J. Power Sources 124 (2003) 65–67.
[9] M. Pastula, J. Devitt, Solid Oxide Fuel Cells VII, vol. 2001-16, Fuel Processing Development at Global Thermoelectric Inc., 2001, pp. 180–189.
[10] Y.P. Chyou, T.D. Chung, C.S. Cheng, T.J. Chen, The 27th Annual Conference of Applied Mechanics, ROC, Taiwan, 2003.
[11] W.H. Lai, T.Y. Tsai, T.S. Chen, Y.T. Lee, The 14th Annual Conference of Combustion Institute, ROC, Tao-Yuan, 2004.
[12] H. Jin, M. Ishida, Int. J. Hydrogen Energy (2000) 1209–1212.